

Scaling Analysis of the Thermal Boundary Layer Adjacent to an Abruptly Heated Inclined Flat Plate

S.C. Saha, C. Lei and J.C. Patterson

School of Engineering
James Cook University, Townsville, QLD 4811, AUSTRALIA

Abstract

The natural convection thermal boundary layer adjacent to an abruptly heated inclined flat plate is investigated through a scaling analysis and verified by numerical simulations. In general, the development of the thermal flow can be characterized by three distinct stages, i.e. a start-up stage, a transitional stage and a steady state stage. Major scales including the flow velocity, flow development time, and the thermal and viscous boundary layer thicknesses are established to quantify the flow development at different stages and over a wide range of flow parameters. Details of the scaling analysis and the numerical procedures are described in this paper.

Introduction Natural convection is a very common phenomenon in nature. Natural convection along an inclined plate has received less attention than the cases of vertical and horizontal plates. However, natural convection heat transfer from an inclined surface is very frequently encountered in engineering devices and the natural environment. A large body of literature exists about an inclined semi infinite flat plate because of its engineering application [1, 2, 10, 12]. Most of the previous works have been conducted by either numerical simulations or experimental observations. Theoretical or scaling analyses have not played a significant role for this type of problem, especially with regard to the transient flow behavior from start up, which is of great fundamental interest and has practical importance. In contrast to the inclined plate problem, very detailed scaling analysis has been carried out for the transient flow in rectangular cavities with differentially heated sidewalls [8], and theoretical analyses of triangular cavities with a sloping bottom have also been reported in the context of natural convection induced circulation in coastal waters [3, 4]

Scale analysis is a cost-effective way that can be applied as a first step in understanding the physics underlying the fluid flow and heat transfer issues. The results of scale analysis can serve as a guide for both experimental and numerical investigations. Therefore, scaling has been used by many researchers to investigate the transient flow development for different kinds of geometries and thermal forcing. Patterson & Imberger [8] carried out an extensive investigation of the transient behavior of natural convection of a two dimensional rectangular cavity in which the two opposing vertical sidewalls are simultaneously heated and cooled by an equal amount. The authors proposed several flow regimes of the transient flow development based on the relative values of the Rayleigh number Ra , the Prandtl number Pr , and the aspect ratio of the cavity A . Schladow, Patterson & Street [11] conducted a series of two- and three- dimensional numerical simulations of the transient flow in a side-heated cavity, and their simulations generally agree with the results of the scaling arguments of Patterson & Imberger [8].

Scaling analyses coupled with numerical simulations have been used in a variety of other geometries and thermal forcing. For example, very recently, Lin & Armfield [5, 6,7] investigated the

transient processes of cooling an initially homogeneous fluid by natural convection in a vertical circular cylinder and in a rectangular container.

To identify possible flow regimes of the unsteady natural convection flow in a small-slope shallow wedge induced by the absorption of solar radiation, Lei & Patterson [3] presented a scaling analysis and established relevant scales to quantify the flow properties in each flow regime. They classified the flow development broadly into one of three regimes: a conductive regime, a transitional regime and a convective regime, depending on the Rayleigh number.

Scaling analysis of the transient behavior of the flow in an attic space was conducted by Poulikakos & Bejan [9], valid for shallow spaces i.e. $H/B \rightarrow 0$, where H and B are the attic height and length respectively. The transient phenomenon began with the sudden cooling of the upper sloped wall. It was noted that both walls developed thermal and viscous layers whose thickness increased towards steady state values. The authors mentioned that, by properly identifying the timescales of various features that develop inside the enclosures, it was possible to predict theoretically the basic flow features that would endure in the steady state. Finally, they focused on a complete sequence of transient numerical simulations covering a range of controlling parameters including the Grashof number, the aspect ratio and the Prandtl number.

In this study, the behavior of the two dimensional transient natural convection flow adjacent to a heated inclined flat plate is investigated by scaling analysis and numerical simulation for Pr less than unity. The scaling analysis is carried out to develop scaling relations for the parameters characterizing the flow behavior at different stages of the flow development. These scaling relations are then validated by a series of numerical simulations with selected values of the Prandtl number (Pr), Grashof number (Gr), and aspect ratio (A) in the ranges of $0.01 \leq Pr \leq 0.72$, $3.59 \times 10^5 \leq Gr \leq 4.24 \times 10^7$ and $0.1 \leq A \leq 1.0$. There is no experimental data available to validate with the numerical and analytical solutions obtained here. Since our aim is to analyze laminar model, we have restricted the range of the Grashof numbers as above.

Problem Formulation

The physical system sketched in Figure 1 consists of an inclined flat plate (AB). We extend both sides of the plate by a distance equal to its length and form a rectangular domain, which is filled with a stationary fluid at a temperature T_c . If we consider the plate as the hypotenuse of a right angled triangle then the altitude is h , the length of the base is l and the angle of the plate, which makes with the base is θ . Except for the plate (the AB section shown in figure 1), all walls of the rectangular domain are assumed to be adiabatic. At the time $t = 0$, the plate is suddenly heated to $T_h = T_c + \Delta T$ and thereafter maintained at this temperature.

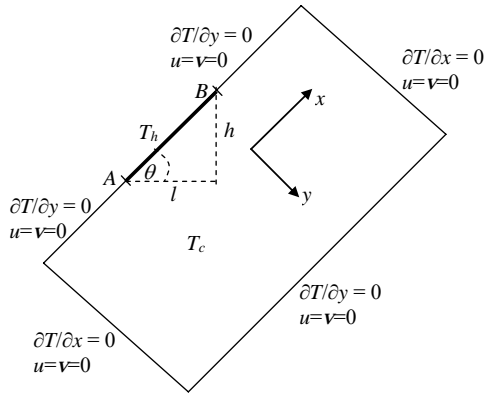


Figure 1. Schematic of the boundary layers developing along the inclined wall.

Under the Boussinesq approximations the governing continuity, momentum and the energy equations take the following forms.

$$\frac{\partial u}{\partial x} + \frac{\partial v}{\partial y} = 0 \quad (1)$$

$$\frac{\partial u}{\partial t} + u \frac{\partial u}{\partial x} + v \frac{\partial u}{\partial y} = -\frac{1}{\rho} \frac{\partial p}{\partial x} + \nu \left(\frac{\partial^2 u}{\partial x^2} + \frac{\partial^2 u}{\partial y^2} \right) + g\beta \sin \theta (T - T_c) \quad (2)$$

$$\frac{\partial v}{\partial t} + u \frac{\partial v}{\partial x} + v \frac{\partial v}{\partial y} = -\frac{1}{\rho} \frac{\partial p}{\partial y} + \nu \left(\frac{\partial^2 v}{\partial x^2} + \frac{\partial^2 v}{\partial y^2} \right) - g\beta \cos \theta (T - T_c) \quad (3)$$

$$\frac{\partial T}{\partial t} + u \frac{\partial T}{\partial x} + v \frac{\partial T}{\partial y} = \kappa \left(\frac{\partial^2 T}{\partial x^2} + \frac{\partial^2 T}{\partial y^2} \right) \quad (4)$$

where u and v are the velocity components parallel and normal to the inclined surface respectively. T is the temperature, p is the pressure, t is the time, g the acceleration due to gravity, θ is the angle of the inclined plate with the horizontal base, and ν , ρ , β and κ the kinematic viscosity, density, coefficient of thermal expansion and thermal diffusivity of the fluid respectively. All fluid properties are evaluated at the temperature T_c .

Scaling Analysis

Thermal Layer Development

The instantaneous heating on the flat plate triggers the transient natural convection phenomenon. A thermal boundary layer develops adjacent to the inclined plate. The energy equation (4) indicates that since the fluid is initially motionless the heating effect of the plate will first propagate into the fluid layer through pure conduction, resulting in a thermal boundary layer of thickness $O(\delta_T)$. Within the boundary layer, the dominant balance is that between the unsteady and diffusion terms in the energy equation (4), giving,

$$\delta_T \sim \kappa^{1/2} t^{1/2} \quad (5)$$

In the momentum equation (2), the unsteady inertia term is of $O(u/t)$, the viscous term $O(\nu u/\delta_T^2)$, and the advection term $O(u^2/AB)$. The ratio of the advection term to the unsteady term is then $O(ut/AB)$. For very small time $ut/AB \ll 1$. Therefore the advection term is not significant for small time. The ratio of unsteady to viscous terms is $(u/t)/(\nu u/\delta_T^2) \sim \delta_T^2/(\nu t) \sim 1/Pr$, where $Pr = \nu/\kappa$. For $Pr \ll 1$ the viscous term is much smaller than the unsteady term, and the correct balance is between the unsteady term and buoyancy. However for $Pr \gg 1$, the unsteady term is much smaller than the viscous term, and the correct balance is between viscosity and buoyancy. If $Pr \sim O(1)$, then the unsteady and viscous terms are of the same order, and thus both terms need to be included in a balance with the buoyancy term.

The unsteady term is $O(u/t)$ and the viscous term is $O(\nu u/t)$, so these two terms together are $O((1 + Pr)u/t)$. Now the balance in the inclined momentum equation is

$$(1 + Pr) \frac{u}{t} \sim g\beta \Delta T \sin \theta$$

Therefore $u \sim g\beta \sin \theta \Delta T t / (1 + Pr) \Rightarrow u \sim g\beta \cos \theta \tan \theta \Delta T t / (1 + Pr)$. The slope or aspect ratio is $\tan \theta = A$ and $\cos \theta = l/(l^2 + h^2)^{1/2} = 1/(1 + A^2)^{1/2}$. Hence,

$$u_i \sim \frac{ARaPr}{(1 + Pr)(1 + A^2)^{1/2}} \left(\frac{t}{h^2/\kappa} \right) \left(\frac{\kappa}{h} \right) \quad (6)$$

where the Rayleigh number is defined as $Ra = g\beta \Delta T h^3 / \nu \kappa$.

As time passes, the boundary layer thickness δ_T continues to grow until a balance between convection and conduction.

$$u \frac{\Delta T}{l/\cos \theta} \sim \kappa \frac{\Delta T}{\delta_T^2} \Rightarrow u \sim \frac{l}{t \cos \theta} \quad (7)$$

Using the velocity scales (6) and (7) we conclude that the growth of the boundary layer along the plate ends at a time of the order

$$t_s \sim \frac{(1 + Pr)^{1/2} (1 + A^2)^{1/2}}{ARa^{1/2} Pr^{1/2}} \left(\frac{h^2}{\kappa} \right) \quad (8)$$

The thickness of the thermal boundary layer along the plate at the steady state time t_s is

$$\delta_T \sim \frac{h(1 + Pr)^{1/4} (1 + A^2)^{1/4}}{A^{1/2} Ra^{1/4} Pr^{1/4}} \quad (9)$$

At the time when the thermal boundary layer reaches the steady state, the u velocity scale is

$$u_s \sim \frac{Ra^{1/2} Pr^{1/2}}{(1 + Pr)^{1/2}} \left(\frac{\kappa}{h} \right) \quad (10)$$

Viscous Layer Development

Concurrently with the formation of a thermal boundary layer, the diffusion of vorticity into the enclosure generates a viscous boundary layer. The thickness δ_v of this viscous layer is a direct result of a balance between the viscous and inertia terms in the momentum equation,

$$\delta_v \sim (\nu t)^{1/2} \sim Pr^{1/2} \delta_T \quad (11)$$

Here it is noted that for $Pr < 1$, viscous boundary layer thickness is smaller than that of the thermal boundary layer. However, the opposite is true when $Pr > 1$. When the thermal layer has reached the steady state, the viscous layer has a thickness of order

$$\delta_v \sim Pr^{1/4} \frac{h(1 + Pr)^{1/4} (1 + A^2)^{1/4}}{A^{1/2} Ra^{1/4}} \quad (12)$$

Numerical Procedure

In order to validate the various scales given in the previous section, a series of numerical simulations have been carried out for the cases described in Table 1. Equations (1) - (4) are solved along with the initial and boundary conditions using the SIMPLE scheme in Fluent 6.3.26, in which the spatial derivatives are discretised with a second order upwind scheme and the diffusion terms with a second order center-differenced scheme. The temporal derivatives are discretized with a second order implicit scheme. To ensure that a sufficiently high accuracy is achieved in the numerical simulations, a non-uniform computational mesh has been used which concentrates points in the boundary layer and near the plate, and is relatively coarse in the interior of the domain. Mesh and time step dependence tests have been carried out for three different inclination angles (aspect ratios). The time steps have been chosen in such a way that the CFL (Courant-Freidrich-Lewy) number remains the same for all meshes.

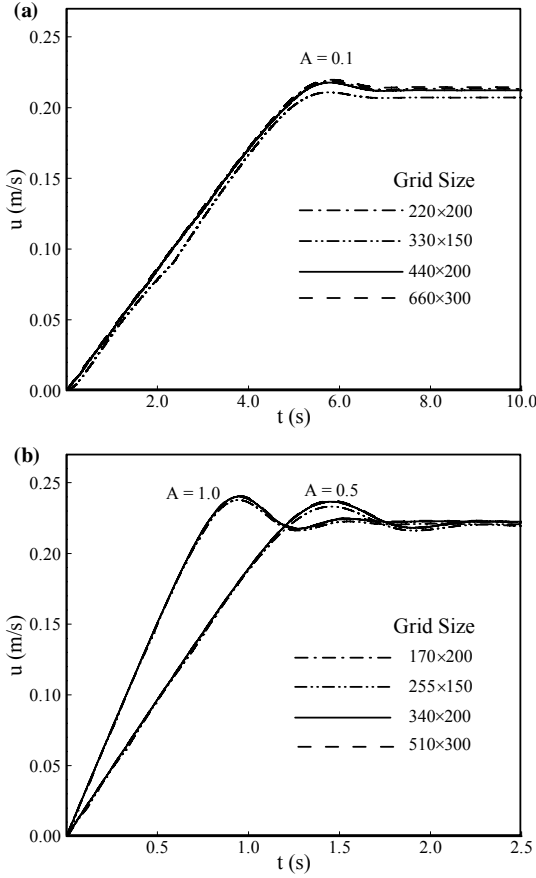


Figure 2: Time series of maximum velocity parallel to the inclined surface calculated on the line normal to the surface at mid point for (a) $A = 0.1$ and (b) $A = 0.5$ and 1.0 , while $Gr = 4.24 \times 10^7$ and $Pr = 0.72$.

A mesh and time step dependence test has been conducted for the highest Grashof number case. It is expected that the selected mesh for the highest Grashof number is appropriate for all the lower Grashof numbers. The time histories of the calculated maximum velocity parallel to the sloping wall with four different meshes are plotted in figure 2. It is seen in this figure that all solutions indicate three stages of the flow development, an initial growth stage, a transition stage and a steady state stage. In the initial growth stage, the four solutions follow each other closely (except for the solution with a coarse mesh 330×150 , which deviates slightly from the other three meshes for $A = 0.1$ in figure 2a). The transition stage is characterized by a single overshoot. The time to reach the steady state is around 1.5s, 2.2s and 7s for $A = 1.0$, 0.5 and 0.1 respectively. The maximum variation of the velocity between the coarsest and finest meshes for $A = 0.1$ is approximately 3.8%, and the maximum variation among the three fine meshes is approximately 1.4%. The maximum variations of the velocity between the coarsest and finest meshes for $A = 0.5$ and 1.0 are 1.3% and 0.4% respectively. Therefore a fine mesh of 440×200 for $A = 0.1$ and a relatively coarse mesh of 340×200 for aspect ratio $A = 1.0$ and 0.5 are adopted for the present simulations.

Validation of the Scaling

The three relations for the steady state boundary layer development can be re-written as

$$\frac{t_s}{h^2 / \kappa} \sim \frac{(1 + Pr)^{1/2} (1 + A^2)^{1/2}}{ARa^{1/2} Pr^{1/2}} \quad (13)$$

$$\delta_T \sim \frac{h(1 + Pr)^{1/4} (1 + A^2)^{1/4}}{A^{1/2} Ra^{1/4} Pr^{1/4}} \quad (14)$$

$$\frac{hu_s}{\kappa Ra^{1/2}} \sim \frac{Pr^{1/2}}{(1 + Pr)^{1/2}} \quad (15)$$

Table 1: Values of A , Gr and Pr for the 12 runs.

Run number	A	Gr	Pr
1	0.5	4.24×10^7	0.72
2	0.5	8.48×10^6	0.72
3	0.5	3.59×10^6	0.72
4	0.5	7.18×10^5	0.72
5	0.5	3.59×10^5	0.72
6	0.5	4.24×10^7	0.5
7	0.5	4.24×10^7	0.1
8	0.5	4.24×10^7	0.05
9	0.5	4.24×10^7	0.025
10	0.5	4.24×10^7	0.01
11	1.0	4.24×10^7	0.72
12	0.1	4.24×10^7	0.72

From Table 1, Runs 1-5 with $Gr = 4.24 \times 10^7$, 8.48×10^6 , 3.59×10^6 , 7.18×10^5 and 3.59×10^5 while keeping $A = 0.5$ and $Pr = 0.72$ unchanged have been carried out to show the dependence of the scaling relations on the Grashof number Gr ; Runs 6-10 with $Pr = 0.5$, 0.1, 0.05, 0.025 and 0.01 while keeping $A = 0.5$ and $Gr = 4.24 \times 10^7$ unchanged have been carried out to show the dependence of the scaling relations on the Prandtl number Pr ; Runs 11-12 and 1 with $A = 1.0$, 0.1 and 0.5 while keeping $Gr = 4.24 \times 10^7$ and $Pr = 0.72$ unchanged have been carried out to show the dependence on the slope, A of the inclination of the plate.

The velocity components and the temperature have been recorded at several locations along a line perpendicular to the plate at the mid point to obtain the velocity and temperature profiles along that line. The maximum velocity parallel to the plate, u_s has been calculated from the velocity components and is used to verify the velocity scale relation.

The thermal boundary-layer thickness δ_T is defined as the perpendicular distance from the mid point of the heated wall to the location where the temperature difference between the fluid in the thermal boundary layer and the ambient drops to $0.01(T_h - T_c)$. The steady state time, t_s for the boundary-layer development to reach the steady state is determined as the moment when the first trough appears in the time history of the u_s maximum parallel velocity along the line perpendicular to the plate at the mid point (see figure 2).

Numerical results of the scaling laws for steady state time, thermal boundary layer thickness and the velocity parallel to the plate, (8), (9) and (10) respectively, are presented in Figure 3. It is seen in the figure that the numerical results agree very well with the scaling relations. For all the calculated cases, the numerical results fall approximately onto a straight line, which proves that the scaling relations (8), (9) and (10) properly describes the thermal boundary layer in the steady state.

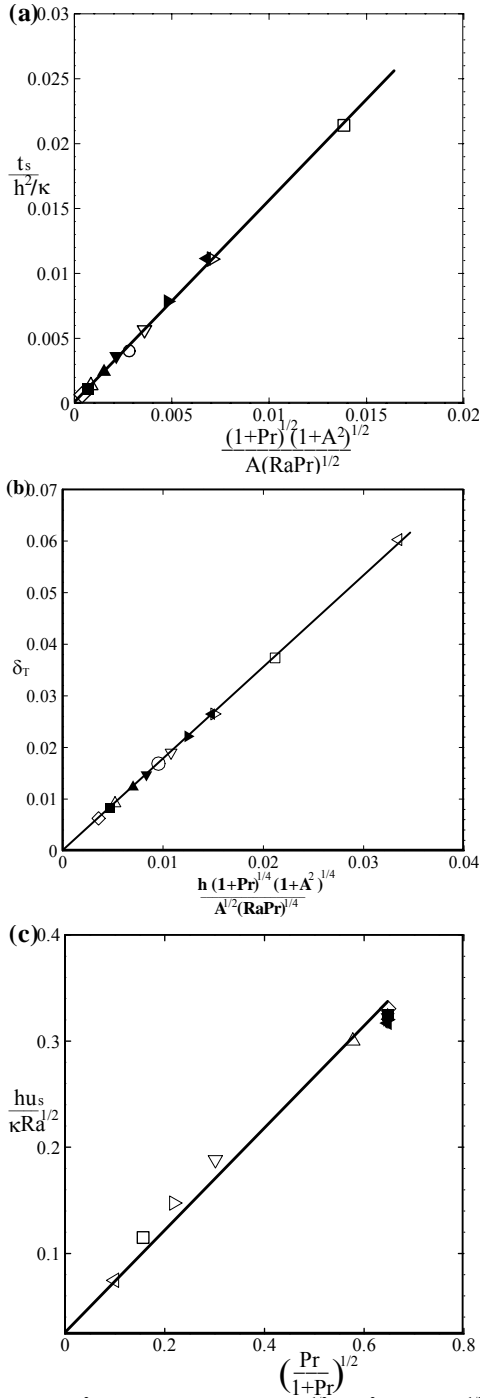


Figure 3. (a) $t_s/(h^2/\kappa)$ plotted against $(1+Pr)^{1/2}(1+A^2)/[A(RaPr)^{1/2}]$; (b) δ_r plotted against $h(1+Pr)^{1/4}(1+A^2)^{1/4}/[A^{1/2}(RaPr)^{1/4}]$; (c) $hu_s/(\kappa Ra^{1/2})$ plotted against $Pr^{1/2}/(1+Pr)^{1/2}$. ■, run 1; ▲, run 2; ▼, run 3; ►, run 4; ◀, run 5; △, run 7; ▽, run 8; ▷, run 9; □, run 10; ◁, run 11, ◇, run 12. Solid line, linear fit.

Conclusions

Natural convection adjacent to a heated inclined flat plate is examined by a scaling analysis and verified by numerical simulations. It is found that the flow is dominated by three distinct stages, i.e. a start-up stage, a transitional stage and a steady stage. Major scaling relations describing the thermal boundary layer adjacent to the heated plate have been established in this study, which are the maximum velocity parallel to the inclined plate inside the boundary layer (u), the time for the boundary layer to reach to the steady state (t_s) and the thermal and viscous boundary layer thicknesses (δ_r and δ_v). Through comparisons of those scaling assumptions with the numerical simulations, it is found that the scaling results agree very well with the numerical simulations. Hence the numerical results have confirmed the scaling relations, which characterize the transient flow development.

Acknowledgments

This research is supported by the Australian Research Council.

References

- [1] Ganesan, P. & Palani, G., Natural convection effects on impulsively started inclined plate with heat and mass transfer, *Heat and Mass Transfer*, **39**, 2003, 277–283.
- [2] Ganesan, P. & Palani, G., Finite difference analysis of unsteady natural convection MHD flow past an inclined plate with variable surface heat and mass flux, *Int. J. Heat Mass Transfer*, **47**, 2004, 4449–4457.
- [3] Lei, C. & Patterson, J. C., Unsteady natural convection in a triangular enclosure induced by absorption of radiation. *J. Fluid Mech.* **460**, 2002, 181–209
- [4] Lei, C. & Patterson, J. C., Unsteady natural convection in a triangular enclosure induced by surface cooling. *International Journal of Heat and Fluid Flow*. **26**, 2005, 307–321
- [5] Lin, W. & Armfield, S. W., Direct simulation of natural convection cooling in a vertical circular cylinder, *Int. J. Heat Mass Transfer*, **42**, 1999, 4117–4130.
- [6] Lin, W. & Armfield, S. W., Natural convection cooling of rectangular and cylindrical containers, *Int. J. Heat Fluid Flow*, **22**, 2001, 72–81.
- [7] Lin, W. & Armfield, S. W., Long-term behavior of cooling fluid in a rectangular container, *Phys. Rev. E.*, **69**, 2004, 05631
- [8] Patterson, J. C. & Imberger, J. Unsteady natural convection in a rectangular cavity, *J. Fluid Mech.*, **100**, 1980, 65.
- [9] Poulidakos, D. and Bejan, A., The fluid dynamics of an attic space, *J. Fluid Mech.*, **131**, 1983, 251–269.
- [10] Said, S. A. M., Habib, M. A., Badr, H. M. & Anwar, S., Turbulent natural convection between inclined isothermal plates, *Computers & Fluid*, **34**, 2005, 1025–1039.
- [11] Schladow, S. G., Patterson, J. C. & Street, R. L., Transient flow in a side-heated cavity at high Rayleigh number: A numerical study. *J. Fluid Mech.*, **200**, 1989, 121–148
- [12] Sparrow, E. M. and Husar, R. B., Longitudinal vortices in natural convection flow on inclined plates, *J. Fluid. Mech.*, **37**, 1969, 251–255.